ISSN 0012-5016, Doklady Physical Chemistry, 2013, Vol. 449, Part 2, pp. 78–82. © Pleiades Publishing, Ltd., 2013.
Original Russian Text © Yu.I. Petrov, E.A. Shafranovsky, N.S. Perov, A.P. Kuznetsov, G.V. Karpov, 2013, published in Doklady Akademii Nauk, 2013, Vol. 449, No. 5, pp. 547–551.

PHYSICAL CHEMISTRY

Magnetism of Aerosol FeCu Nanoparticles in a Wide Concentration Range

Yu. I. Petrov[a], E. A. Shafranovsky[a], N. S. Perov[b], A. P. Kuznetsov[b], and G. V. Karpov[a]

Presented by Academician A.A. Berlin September 10, 2012

Received September 12, 2012

DOI: 10.1134/S0012501613040076

Metastable FeCu alloys, fabricated by rapid melt quenching or ball milling, are of considerable scientific and applied interest. Their unique properties, mainly caused by the insolubility of the components in each other at room temperature, have been addressed in a great number of works (see, e.g., references in [1]). However, contradictory data on the alloy structure and composition have been reported. In addition, some problems remain unclear. For example, no consensus has been achieved concerning the existence and role of the high-temperature γ-Fe modification in metastable FeCu alloys.

To resolve these contradictions, the structure and magnetic states of the aerosol FeCu particles containing 0.6–92.1 at % Cu obtained by the gas condensation method [2] have been studied by, respectively, X-ray diffraction and Mössbauer spectroscopy [1]. A unique feature of this method is the possibility to freeze the high-temperature states of particles upon their rapid cooling in an inert gas. In addition, since the particles are small, their equilibrium state can be achieved due to fast atomic diffusion. It has been shown that the particles have an iron core surrounded by a shell composed of copper and iron and copper oxides. The particles containing 50.4 at % Cu have the core 12–15 nm in diameter (d) and the average outer diameter D of about 24 nm. With an increase in the copper content, such a core, which has a bcc structure with a noticeably increased lattice parameter (as compared with that of pure iron) caused by the embedment of the copper atoms, decreases until it disappears, and simultaneously the ferromagnetism of the particles vanishes.

Within the range of $c = 4.9–74.3$ at % Cu, the bcc and fcc phases coexist. The fcc phase has a pure copper structure with a slightly increased lattice parameter due to the embedment of Fe atoms. In iron-rich particles, two γ-Fe states—ferromagnetic and paramagnetic—are present. For FeCu particles with $c = 4.9$ at % Cu, which have a thin copper shell, only the ferromagnetic state is observed. As the shell becomes thicker, this ferromagnetic state is enhanced. However, it exists only in few layers adjacent to copper, and the next layers are paramagnetic. Therefore, in addition to the ferromagnetic state of γ-Fe, its paramagnetic state appears as well. Owing to the copper oxidation in thicker shells, the formation of the fcc lattice of γ-Fe is hindered so that both states of this iron modification gradually disappear in the range $19.7 < c < 35.3$ at % Cu. At the same time, at $c \geq 35.3$ at % Cu, small isolated aggregates of iron atoms appear in the samples, the former giving rise to a paramagnetic singlet in Mössbauer spectra. The particles containing above 80 at % Cu have a fcc structure and are paramagnetic. A certain fraction of their paramagnetism is presumably caused by the Fe atoms in the copper lattice.

Additional information on the magnetic properties of deposited aerosol particle can be obtained from hysteresis loop analysis. In this work, the hysteresis loops have been measured for the first time for aerosol FeCu nanoparticles in a wide composition range deposited onto glass. The change in the shape of these loops with an increase in the copper content allows us to judge the particle interaction mechanisms. Initial FeCu alloys containing 4.9–92.1 at % Cu were prepared by means of a VChG 4/10-0.44 high-frequency generator (working frequency, 440 kHz) by direct alloying of carbonyl iron and electrolytic copper levitated in an argon flow at atmospheric pressure in a specially designed counterflow inductor. After melting, the alloy components were rapidly mixed by eddy currents. Then, the generator was switched off, and the molten drop fell into a massive copper vessel.

To prepare aerosol particles, FeCu alloy billets of 100–150 mg in weight were fixed on a tungsten vaporizer in a vacuum chamber and degassed by heating at a pressure of less than 10^{-3} Torr. Then, the setup was filled with argon to a pressure of 3 Torr, and the billets were rapidly vaporized. Emerging aerosol particles were deposited onto cover glasses suspended near the

[a] *Semenov Institute of Chemical Physics, Russian Academy of Sciences, ul. Kosygina 4, Moscow, 119991 Russia*
[b] *Moscow State University, Moscow, 119991 Russia*

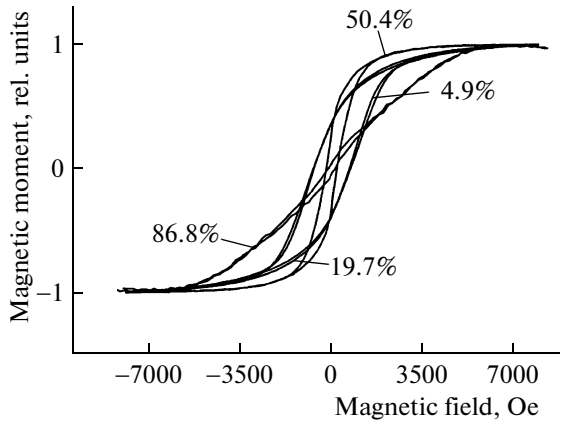

Fig. 1. Hysteresis loops of FeCu particles with a different copper content deposited on cover glass (LakeShore 7407 VSM instrument).

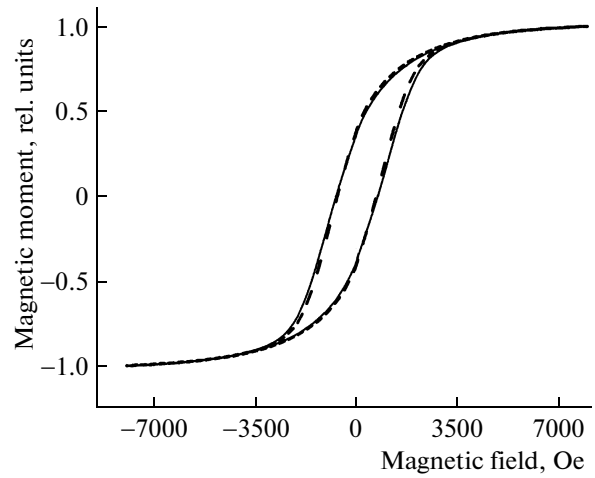

Fig. 2. Hysteresis loops of FeCu(19.7 at %) particles on cover glass (LakeShore 7407 VSM instrument) measured for two orientations of the magnetic field relative to the sample plane.

inner wall of a cylinder 10 cm in diameter at different distances from the vaporizer. According to transmission electron microscopy (TEM) data, the deposited particles were spherical with the average diameter $D \approx 24$ nm and a narrow size distribution at any composition. In the course of formation, particles were cooled and combined into chains of different length under the action of magnetic forces when their temperature turned out to be below the Curie temperature. Because of the different thickness of the deposits, their color varied from gray to black. To prevent self-ignition of the as-prepared powders in air, the samples were kept for 12 h in the residual gas atmosphere of the vacuum setup [3]. Pure iron particles with the core size $d \approx 15$ nm deposited on cover glass were prepared analogously.

Magnetic measurements were made with a vibrating sample anisometer (VSA) and a LakeShore 7407 vibrating sample magnetometer (VSM). Typical hysteresis loops for samples with different copper contents are shown in Fig. 1. As is seen, with an increase in the copper content, the hysteresis loop shape changes (the coercive force and saturation field decrease). Figure 2 shows normalized hysteresis loops of particles with the copper content 19.7 at % measured at two magnetic field orientations: parallel (solid line) and perpendicular (dashed line) to the sample plane. For both orientations, measurements were taken twice with in-plane 90° rotation of the sample. When the field orientation is perpendicular to the sample plane, the coercive force was a few percent lower. Such a behavior is typical of the magnetization along the hard anisotropy axis. The normalized hysteresis loops are almost coincident, which is evidence that the deposit is isotropic. An analogous behavior is observed for the other samples.

From the hysteresis loop, we can determine the coercive force (H_c) necessary for demagnetization of the sample ($M = 0$), the switching field H_{sw} at the point where the loop branches merge with each other (the field above which there are only reversible remagnetization processes accomplished by rotation of the magnetization vector of separate particles), and the H_s field at which the magnetic saturation of the sample (M_s) is achieved. Figure 3 shows the plot of H_c versus the particle composition calculated from the hysteresis loops of the samples. For each composition, four samples (eight samples of pure iron) located at different distances from the vaporizer were used, which was responsible for different deposition conditions (different sample thicknesses and random configurations of particle chains) and led to some data scatter.

Figure 3 shows the average H_c values, as well as their root-mean-square deviations. Within the data scatter, the results obtained with the VSA and VSM LakeShore 7407 setups coincide. For the magnetic field oriented parallel to the sample plane, the plot of H_c versus concentration first decreases from 1300 Oe for pure iron to $H_c = 800$ Oe at $c = 4.9$ at % Cu then slightly increases to $H_c \approx 1000$ Oe at $c = 35.3$ at % Cu, and sharply decreases to a minimum ($H_c \approx 100$ Oe) for FeCu (50.4 at %) particles. As the copper content further increases, a small maximum ($H_c = 220$ Oe) is observed near $c = 74.3$ at %. When the magnetic field is perpendicular to the sample plane, the concentration dependence of H_c has the same shape as in the case of the parallel orientation, but the H_c values are slightly lower.

Figure 4 shows the concentration dependence of the uniaxial anisotropy constant (K) for deposited FeCu particles calculated by the equations

$$K = H_a M_s/2, \quad (1)$$

$$H_a^2 = 15H^2 \frac{M_s - M}{M_s}, \quad (2)$$

where $H_a = 2K/M_s$ is the anisotropy field.

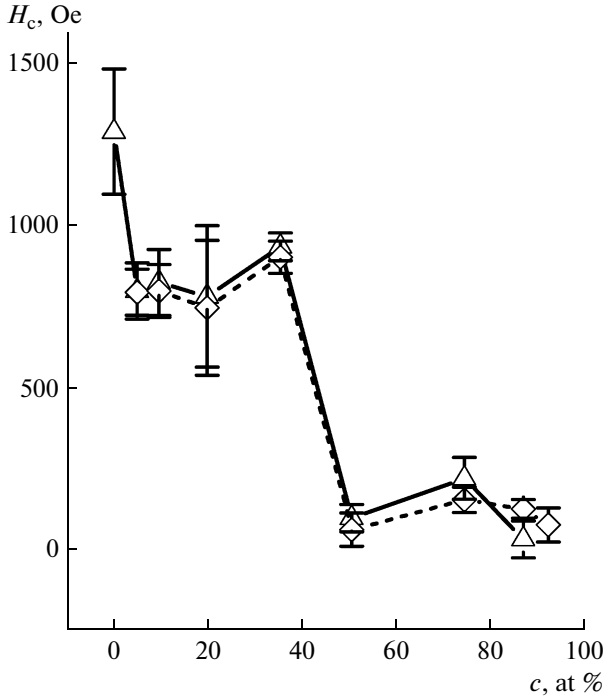

Fig. 3. Concentration dependence of the coercive force (H_c) for two orientations of the magnetic field relative to the sample plane.

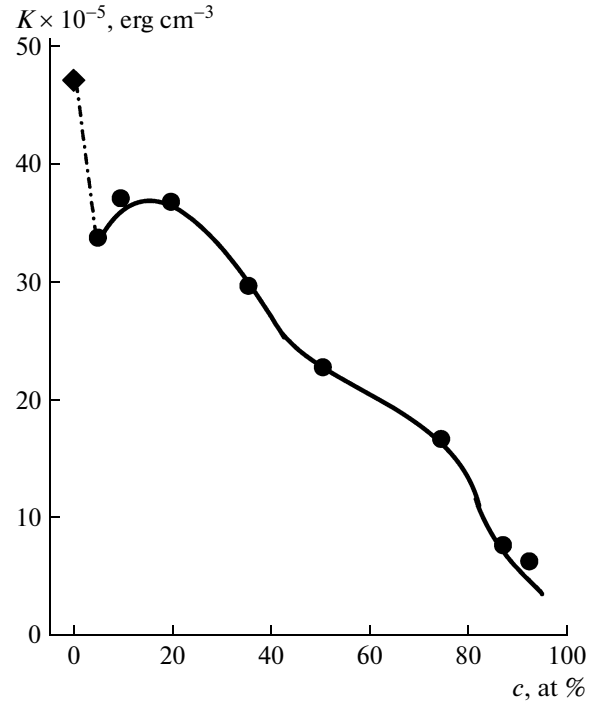

Fig. 4. Concentration dependence of the uniaxial anisotropy constant (K) for FeCu deposits of different composition: ● this work, ◆ anisotropy constant of Fe particles [3] prepared under the same conditions as FeCu particles in this work.

According to the Stoner–Wohlfarth model [4] for an ensemble of noninteracting identical single-domain particles, there is a barrier between two easy magnetization directions, $E_K = KV\sin^2\varphi$, where V is the particle volume, and φ is the angle between its magnetization (I_s) and the nearest easy magnetization axis. These directions are specified by the potential energy minima of the particle. The E_K barrier prevents the transition of I_s from one minimum to the other. In addition, this barrier determines the K constant. Beck was the first to express the magnetic energy of a crystal through the anisotropy constant and direction cosines of the I_s vector on the basis of semiempirical consideration [5]. Later [6], Akulov has developed the strict theory of crystallographic anisotropy, using the matrix transformation of vectors for crystals of different symmetry. The symmetry characterizes the internal structure of the crystal and depends on neither its shape nor the external magnetic field.

By contrast, the uniaxial anisotropy depends on the particle shape, being maximal for a prolate ellipsoid or a needle. The uniaxial anisotropy appears in relatively strong magnetic fields H when the magnetization I_s of the particles turns out to be close to the H direction. The vector transition from one potential energy minimum to the other can be caused by thermal fluctuations, magnetic field, or crystal distortions. In particular, this transition is accompanied by small Barkhausen jumps in the curve of magnetization versus H. If the easy magnetization axes of separate particles coincide with the field H, the hysteresis loop has a rectangular shape [4]. Otherwise, the hysteresis loop is inclined [3, 4]. This is precisely what is observed for deposits of aerosol particles chaotically oriented on the substrate (Figs. 1 and 2).

The anisotropy field H_a is commonly calculated by Akulov's equation (2), which describes the approach of hysteresis loops to saturation for noninteracting single-domain particles [6]. However, the relationship $H_a = 2K/M_s$ is also applicable for interacting particles if H_a is taken to be H_{sw} [3].

In some works, the Stoner–Wohlfarth model taking into account the presence of both the uniaxial and cubic magnetic anisotropy of particles in combination with Akulov's equation is experimentally supported, for example, in measurements of hysteresis loops of Fe_3C [7] and $Co_{1-x}Ni_x$ ($x = 0$–1) [8] particles encapsulated into carbon nanotubes. It has been stated in [8] that single-domain CoNi (as well as Fe_3C) particles in carbon nanotubes do not interact with each other and, hence, have high anisotropy constants $K = (15.2$–$27.1) \times 10^5$ erg cm^{-3} for different CoNi compositions. The authors attribute the high anisotropy constants to the prolate shape of particles [8], although this conclusion has not been confirmed by the TEM images of Fe_3C particles [7]. It is evident that the difference in K values is most likely due to the interaction of particles in the samples since the image shows clearly pronounced chains of two and more spherical particles.

The strongly enhanced anisotropy of single-domain particles has been repeatedly reported [3, 9–13]. This has been surprising for some researchers [11]. Other researchers have explained the high uniaxial anisotropy of the particles as compared with the crystallographic anisotropy of iron by the induced interaction between the ferromagnetic core and ferri- or antiferromagnetic oxide shell of the particles. If this were the case, a large hysteresis loop displacement would be observed. However, attempts have been unsuccessful to reveal such an effect by hysteresis loop measurements for iron particles with $D = 20$ nm [13] and by ferromagnetic resonance ($D = 50$ nm) [14]. The small bias of the hysteresis loop from 100 Oe at room temperature to 200 Oe at 10 K has been observed for aerosol iron particles ~11 nm in diameter coated with amorphous Fe_3O_4; however, this bias vanishes upon oxide crystallization after heating [3]. Simultaneously, the passivating effect of the amorphous oxide shell is eliminated. It is evident that the lack of the hysteresis loop bias for larger particles is also related to the Fe_3O_4 oxide crystallization.

The most plausible explanation of the high coercive force and uniaxial anisotropy, suggested by Jacobs and Bean [9], implies the formation of chains of single-domain particles. Calculations have shown that chains comprising two or three particles suffice to result in the observed increase in the coercive force H_c and the uniaxial anisotropy constant K [9, 10]. However, only the experiment can give the answer to the question about the magnetism of chains of particles separated by different interlayers. In this paper, we report the result of magnetic measurements of chains of FeCu particles with the iron core coated with a layer of iron oxides, as well as copper and its oxides, the composition of the layer changing with an increase in the copper content in the particles.

A complex character of the dependence of H_c on the copper content in the particles (Fig. 3) is evidently a result of the interplay of different factors that can both enhance and suppress the interaction between the particles. The scatter of the H_c values for the samples located at different distances from the vaporizer can be attributed to some change in the deposit thickness and particle size distribution. It is well known that, as the average diameter D of iron particles decreases, the coercive force first increases to H_c = 1000–1200 Oe at $D \approx 20$ nm, which is close to the theoretically found size (D_0) of single-domain particles, and then sharply decreases [3, 10, 15]. The particles with $D < D_0$ retain their single-domain structure since the Bloch wall width (≈15 nm) required for their magnetization reversal exceeds the particle size. In this case, the decrease in H_c is related to the particle size distribution.

It is worth noting that the coercive force is determined only by those particles that have the volume V exceeding the blocking volume at a given temperature V_b, which accounts for the sharp boundary of their transition to the superparamagnetic state. A specified particle size distribution has both the superparamagnetic ($V < V_b$) and ferromagnetic ($V > V_b$) particles. Superparamagnetic particles do not make contribution to H_c. If the volume of particles of average size is smaller than V_b, the majority of them will be superparamagnetic. Simultaneously, the ferromagnetism of the sample becomes weaker because of a small number of particles corresponding to the distribution tail some of which have a multidomain structure at $D > D_0$. In such particles, there is a decrease in H_c caused by the generation of energetically favorable closed magnetic fluxes.

The coercive force H_c depends not only on the particle size but also on the anisotropy of the shape of separate particles, as well as on the anisotropy caused by the aggregation of these particles into chains. However, the character of their interaction in the chains is different for iron and FeCu deposits. Even in the course of preparation of FeCu(<35.3 at %) particles, ferromagnetic γ-Fe layers can appear on their copper shell, and these layers ensure the rigidity and stability of chains of different length. The magnetic properties of such chains depend on the particle composition.

The concentration dependence of H_c at $c <$ 35.3 at % (Fig. 3) can be explained by the interplay between two opposite factors, one of which decreases and the other increases H_c with an increase in the copper content in the particles. The decrease in H_c (as compared with pure iron) is caused by the appearance and thickening of copper interlayers between the particles in the chains, whereas the growth of ferromagnetic γ-Fe on the forming copper lattice increases H_c. As a result, the concentration dependence curve has a minimum near $c \approx 5$ at %. At $c < 5$ at %, the effect of copper layer thickening prevails over the effect of γ-Fe. Inasmuch as the H_c minimum is independent of the sample orientation in the magnetic field, this is evidence that the spatial anisotropy of the arrangement of particle chains is unnoticeable. At the same time, the gradual increase in the coercive force to the maximum as the copper concentration changes from 5.0 to 35.3 at % is presumably related to the increase in the chain length. The subsequent decrease in H_c to the minimum (98 Oe) for the FeCu(50 at %) particles is caused by the gradual disappearance of γ-Fe as a result of copper oxidation and progressive thickening of the nonmagnetic shell of the particles, as well as due to the corresponding decrease in the size of the iron core. This leads to the weakening of the interaction between the particles and hinders the formation of chains upon generation and primary oxidation of particles in argon. The small H_c maximum at 74.3 at % Cu is likely caused by separate iron clusters on copper grains.

The concentration dependences of H_c (Fig. 3) and the uniaxial anisotropy constant K (Fig. 4) are similar, which is quite natural since both are mainly determined by the character of the chain structure of the deposits.

In conclusion, it should be noted that, in this work, the role of nanoparticle chains and the γ-Fe structure in the magnetism of aerosol FeCu particles of different composition deposited on glass has been comprehensively studied for the first time. The trend of the curve of H_c with an increase in the copper content is caused by two opposite factors: the weakening of the interaction between the particles in the chains as a result of thickening of their nonmagnetic shells and the enhancement of this interaction owing to the ferromagnetic layer of γ-Fe. According to Mössbauer spectra, γ-Fe exists on the surface of the copper shell of particles in the range 4.9–35.3 at % Cu. Its ferromagnetism first increases to the maximum at $c \approx 20$ at % and then gradually decreases due to the transition of γ-Fe to the paramagnetic state, which disappears near $c \approx 35$ at %. This is responsible for the appearance of extrema in the initial segment of the concentration dependence of the coercive force of the samples. With an increase in the copper content, H_c first rapidly decreases to the minimum at $c \approx 5$ at %, then increases to the small maximum at $c = 35.3$ at %, and sharply decreases to the value characteristic of massive iron at $c = 50.4$ at % (Fig. 3). The decrease in H_c is exclusively due to the weakening of the interaction of particles in the chains caused by both the decrease in the iron core size and the thickening of the nonmagnetic oxide core of the particles.

ACKNOWLEDGMENTS

This work was supported by the Russian Foundation for Basic Research (project no. 11–02–90493-Ukr_f_a).

REFERENCES

1. Shafranovsky, E.A., Petrov, Yu.I., Casas, Ll., and Molins, E., *J. Nanopart. Res.*, 2011, vol. 13, pp. 4913–4928.
2. Petrov, Yu.I. and Shafranovskii, E.A., *Bull. Russ. Acad. Sci. Rhys.,* 2000, vol. 64, no. 8, pp. 1236–1244.
3. Shafranovsky, E.A. and Petrov, Yu.I., *J. Nanopart. Res.*, 2004, vol. 6, pp. 71–90.
4. Stoner, E.C. and Wohlfarth, E.P., *Phil. Trans. Roy. Soc. A* (London), 1948, vol. 240, pp. 599–642.
5. Beck, K., Dissertation, Zürich, 1918.
6. Akulov, N.S., *Ferromagnetizm* (Ferromagnetism), Moscow: GITTL, 1939.
7. Komogortsev, S.V., Iskhakov, R.S., Balaev, A.D., et al., *Fiz. Tverd. Tela,* 2007, vol. 49, pp. 700–703.
8. Komogortsev, S.V., Smirnov, S.I., Momot, N.A., and Iskhakov, R.S., *J. Sib. Fed. Univ. Math. Phys.*, 2010, vol. 3, pp. 515–520.
9. Jacobs, I.S. and Bean, C.P., *Phys. Rev.*, 1955, vol. 100, pp. 1060–1067.
10. Petrov, Yu.I., *Fizika malykh chastits* (Physics of Small Particles), Moscow: Nauka, 1982.
11. Ibusuki, T., Kojima, S., Kitakami, O., and Shimida, Y., *IEEE Trans. Magn.*, 2001, vol. 37, pp. 2223–2225.
12. Papaefthymiou, V., Kostikas, A., Simopoulos, A., et al., *J. Appl. Phys.,* 1990, vol. 67, pp. 4487–4489.
13. Meiklejohn, W.H., *J. Appl. Phys.*, 1958, vol. 29, pp. 454–455.
14. Petrov, Yu.I., Rusin, B.A., and Fedorov, Yu.I., *Fiz. Met. Metalloved.*, 1967, vol. 23, pp. 504–510.
15. Petrov, Yu.I., *Klastery i malye chastitsy* (Clusters and Small Particles), Moscow: Nauka, 1986.

Translated by G. Kirakosyan